Journal of the Korean Chemical Society
2009, *Vol. 53, No. 1*
Printed in the Republic of Korea

망간이 혼입된 층상구조 $Na_{1.9}Li_{0.1}Ti_3O_7$ 세라믹스의 유전율 - 분광법과 교류 전도도 측정 연구

Dharmendra Pal*, J. L. Pandey†, and Shripal‡
Department of Applied Physics, Krishna Girls Engineering College, Kanpur-209217, India
†*National Physical Laboratory, New Delhi-110012, India*
‡*Department of Physics, P.P.N. College, Kanpur-208001, India*
(2008. 2. 11 접수)

Dielectric-Spectroscopic and ac Conductivity Investigations on Manganese Doped Layered $Na_{1.9}Li_{0.1}Ti_3O_7$ Ceramics

Dharmendra Pal*, J. L. Pandey†, and Shripal‡
Department of Applied Physics, Krishna Girls Engineering College, Kanpur-209217, India
†*National Physical Laboratory, New Delhi-110012, India*
‡*Department of Physics, P.P.N. College, Kanpur-208001, India*
(Received February 11, 2008)

요 약. 유전율-분광법과 교류 전도도 측정 연구를 망간이 혼입된 층상구조의 $Na_{1.9}Li_{0.1}Ti_3O_7$에 시도하였다. 373-723K 온도와 100Hz-1MHz 주파수 영역에서 loss 탄젠트 (Tanδ), 상대적 유전율 (ε_r) 그리고 교류 전도도 (σ_{ac})의 의존성을 혼입 유도체들에 대하여 조사하였다. 다양한 전도도 메커니즘이 존재하는데 MSLT-1과 MSLT-2의 경우에는 낮은 온도영역에서 전자에 의한 전도도를 보인다. MSLT-3의 경우에는 금지된 층간 이온 전도도가 전자 전도도와 함께 존재한다. 이러한 층간 이온 전도도는 모든 혼입 유도체들에 대하여 중간 온도 영역에 존재한다. 가장 높은 온도 영역에서는 MSLT-1과 MSLT-2의 경우에는 이온 전도도와 polaron에 의한 전도도가 존재하고 MSLT-3에 대하여는 이온 전도도 만이 존재한다. 망간이 혼입된 층상구조의 $Na_{1.9}Li_{0.1}Ti_3O_7$에서 Loss 탄젠트 (Tanδ)는 전자 전도도와 쌍극자의 위치, 그리고 공간 전하 분극화에 기인한다. 상대적 유전율의 증가는 층간에 쌍극자 수의 증가에 기인하고 반면 상대적 유전율의 감소는 높은 혼입율에 따른 누전 전류의 증가에 기인한다.

주제어: Mn 혼입 층상 산화 티타늄 세라믹스, 유전성 성질, 폴라론 전도도, 이온전도도

ABSTRACT. The dielectric-spectroscopic and ac conductivity studies firstly carried out on layered manganese doped Sodium Lithium Trititanates ($Na_{1.9}Li_{0.1}Ti_3O_7$). The dependence of loss tangent (Tanδ), relative permittivity (ε_r) and ac conductivity (σ_{ac}) in temperature range 373-723K and frequency range 100Hz-1MHz studied on doped derivatives. Various conduction mechanisms are involved during temperature range of study like electronic hopping conduction in lowest temperature region, for MSLT-1 and MSLT-2. The hindered interlayer ionic conduction exists with electronic hopping conduction for MSLT-3. The associated interlayer ionic conduction exists in mid temperature region for all doped derivatives. In highest temperature region modified interlayer ionic conduction along with the polaronic conduction, exist for MSLT-1, MSLT-2, and only modified interlayer ionic conduction for MSLT-3. The loss tangent (Tanδ) in manganese-doped derivatives of layered $Na_{1.9}Li_{0.1}Ti_3O_7$ ceramic may be due to contribution of electric conduction, dipole orientation, and space charge polarization. The corresponding increase in the values of relative permittivity may be due to increase in number of dipoles in the interlayer space while the corresponding decrease in the values of relative permittivity may be due to the increase in the leakage current due to the higher doping.

Keywords: Mn-doped Layered titanium oxide ceramics, Dielectric Properties, Polaronic Conduction, Ionic Conduction

INTRODUCTION

The series of titanates with chemical formula $Na_2Ti_nO_{2n+1}$, to which $Na_2Ti_3O_7$ belongs, has a zig zag layer structure.[1,2] O. V. Yakubovich and V. V. Kireev have studied the refined crystal structure of $Na_2Ti_3O_7$.[3] It has been reported that $Na_2Ti_3O_7$ has the ability to decompose water to hydrogen and oxygen when ruthenium oxide is highly disperse on the titanates.[4] In the recent work, synthesis and characterization of $Na_2Ti_3O_7$ and $Na_2Ti_6O_{13}$ reported in the literature.[5] Machida et al.[6] have reported pillaring and photocatalytic properties of partially substituted layered titanates $Na_2Ti_{3-X}M_XO_7$ and $K_2Ti_{4-X}M_XO_9$ (M = Mn, Fe, Cu, Co and Ni). Kikkawa et al. have studied the AC conductivity measurements of $Na_2Ti_3O_7$, $K_2Ti_4O_9$ and their niobium-substituted product.[7] EPR, Dielectric-spectroscopic, ac and dc conductivity investigations of Li, K substituted and paramagnetic ions (Mn, Cu, Fe) doped layered polycrystalline $Na_2Ti_3O_7$ and $K_2Ti_4O_9$ reported by Shripal et al.[8-17] EPR studies of iron and manganese doped tritanates have reported by Alka Tangri et. Al.[50] These titanates have a kind of typical oxides with layered structures and studied extensively as ion exchanger,[18-21] metal ion absorbent[22] and filters in rein-forced plastics.[23] These materials also investigated for intercalation with alumina, slica, chromia and iron oxide to improve their catalytic properties and stability.[24-28] These materials used to fabricate porous materials and to fix radioactive metal ions.[29,30] These compounds have also investigated for their electrochemical and calorimetric thermo dynamical properties.[31] A total of about 130 phases (mostly non-stoichiometric) including a dozen of Sodium titanates have known.[32-35] M. Sh. Khalil and F. F. Hammad have reported effect of Cu addition on structural and dielectric properties of CaTiO3.[36] Structural and morphological behavior of TiO_2 rutile has obtained by the hydrolysis reaction of $Na_2Ti_3O_7$.[37]

No attempt has been made through dielectric-spectroscopic and ac conductivity studies of pure and manganese doped Sodium Lithium trititanate. In the present paper, we have firstly studied about the dielectric-spectroscopic and ac conductivity investigations of manganese doped layered $Na_{1.9}Li_{0.1}Ti_3O_7$ ceramics.

EXPERIMENTAL

The ceramic sample $Na_{1.9}Li_{0.1}Ti_3O_7$ (denoted as SLT) [16] and its manganese-doped derivatives with different molar percentage of MnO_2 (0.01, 0.1 and 1.0) (denoted as MSLT-1, MSLT-2 and MSLT-3) have synthesized using sintering process. The method of preparation of palletized ceramic samples is similar to that reported earlier in the literature.[14] Iso-Debyeflex 2002, Richseifert and Co. differactometer using Cu Kα radiation generated at 30 kV and 20 mA, collected XRD-patterns for all the compositions. The formation of these titanates (MSLT-1, MSLT-2 and MSLT-3) confirmed by the XRD-patterns obtained at room temperature (RT).

The flat faces of the sintered pellets were painted with an air-dried high purity silver paste and then mounted in the sample holder evacuated up to 10^{-3} mbar for the electrical measurements. The loss tangent (tanδ) and parallel capacitance (C_p) of the palletized samples directly measured as a function of temperature and frequency by the HP 4194A impedance analyzer. The relative permittivity (ε') and the bulk a. c. conductivity (σ) of the samples calculated by using formula as reported earlier.[14]

RESULTS AND DISCUSSION

The Ti-O skelton of $Na_2Ti_3O_7$ [*Fig.* 1(a)] consists of TiO6 octahedrons, which share edges and corner. However, the positions of Na^+ ions are very different for the titanate. The Na^+ cations located between the layers neutralize the ionic two dimensional titanium-oxygen constructions. The Na(1) and Na(2) atoms are located in the center of nine and seven vertex oxygen polyhedron, respectively. The cation-oxygen interatomic distance in Na(1)-polyhedron vary over a wider range (2.238-2.961Å the average value is 2.792Å). The Na-O band length in $Na_2Ti_3O_7$ is well above 2Å. Its crystal structure

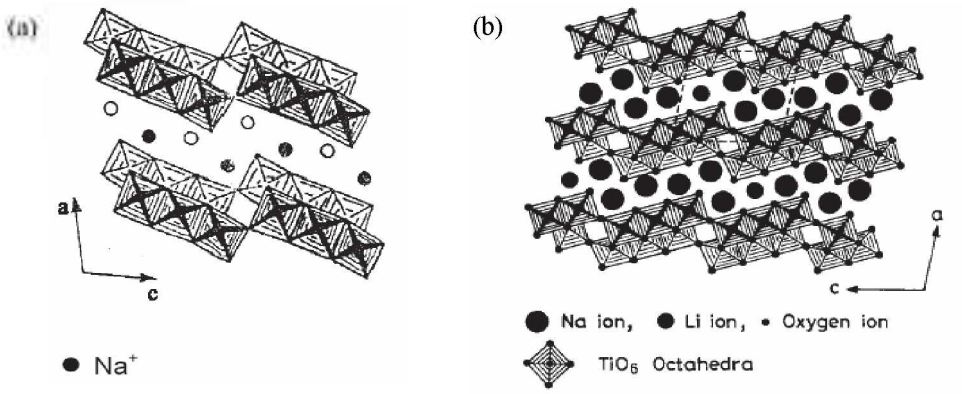

Fig. 1. (a) Idealized structure of $Na_2Ti_3O_7$, Edge shared rectangular unit and sphere represent TiO_6 octahedron and Na atom respectively.[19] (b) Idealized structure of $Na_{2-X}Li_XTi_3O_7$ where X= 0.1 Edge shared rectangular unit and sphere represent TiO_6 octahedron and Na atom respectively[16]

consists of layers of composition $Ti_3O_7^{2-}$, like a two dimensional sheet cantered on the (100) plane. The layers are held together by Sodium ions. The Sodium ions exist in two. different kinds of crystallographic sites. The $Na_2Ti_3O_7$ crystals are monoclinic with unit cell dimensions a=9.133(2)Å, b=3.806(1)Å, c=8.566(2)Å and β=101.57(3)°, space group=$P2_1/m$. The basic framework of $Na_2Ti_3O_7$ is block of TiO_6 octahedra. three at one level three at a distance b/2 Á above and below which are joined through common edges.[1] The substitution of Lithium ions in the interlayer space does not affect the crystal structure of $Na_2Ti_3O_7$. This confirms the presence of small Lithium ions with large Sodium ions in interlayer space. The crystal structure of $Na_{1.9}Li_{0.1}Ti_3O_7$ is shown in *Fig.* 1(b). which indicates that Lithium atoms are accommodated with sodium atoms in widely opened interlayer space. Dotted line represents the unit cell.

The dependence of Loss Tangent (Tanδ) for MSLT-1, MSLT-2 and MSLT-3 in temperature range 373-723K at some fixed frequency is shown in *Figure* 2(a)-(c). The values of tanδ remain invariant up to 398K for MSLT-1, 423K for MSLT-2 and up to 598K for MSLT-3. Above these temperatures the values of tanδ furnishes two relaxations peaks at 598K and 723K for MSLT-1. MSLT-2 and MSLT-3. Above these temperatures the values of tanδ up to the temperature range of study increases sharply at lower frequency and gradually at higher frequency. Generally, the values of tanδ increase appreciably when temperature rises. This growth in tanδ brought about by an increase both in conduction of residual current and the conduction of

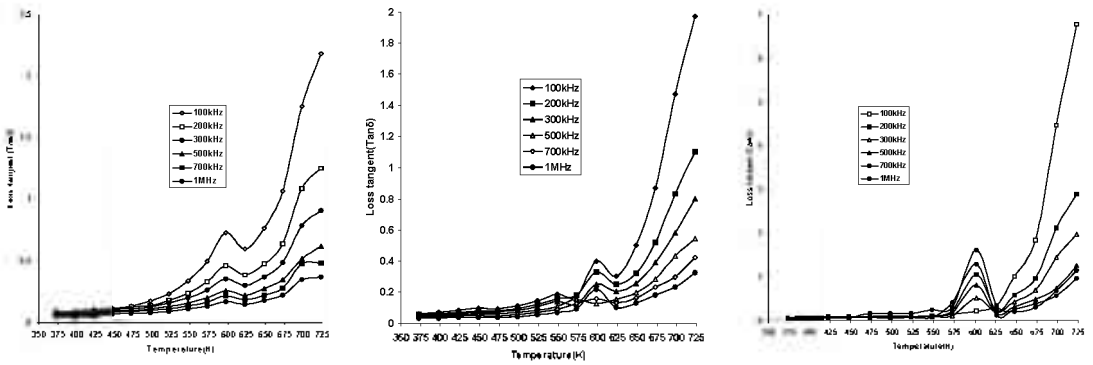

Fig. 2. (a) Loss tangent (Tanδ) versus temperature for MSLT-1. (b) Loss tangent (Tanδ) versus temperature for MSLT-2. (c) Loss tangent (Tanδ) versus temperature for MSLT-3

absorption currents. The losses caused by dipole mechanism reach their maximum at certain definite temperature T_k.[38] However, in actual facts, the rise in temperature and the resulting drop in viscosity exert a double effect on the amount of losses due to the friction of the rotating dipoles. On one hand, degree of dipole orientation increases and on the other hand, there is a reduction in energy required to overcome the resistance of the viscous medium (internal friction of matter) when the dipole rotates through the unit angle. The first factor increases the losses and second diminishes these values.[38] It can proposed that mainly two components are responsible for the dependence of tanδ on temperature and frequency simultaneously:

(i). Firstly, the large losses due to dipole relaxation polarization as relaxation peaks indicated in the high temperature region. However, non-occurrence of any pronounced peak in *Fig.* 2(c) might be because the participating ions in the relaxation polarization grow with rise in temperature. This suppresses all types of relaxation peaks in tanδ versus temperature plots for MSLT-3.

(ii) Secondly, the losses are due to the motion of loosely bound (Na^+ and Li^+) cations in the interlayer space and regarded as a loss due to electrical conduction.

The occurrence of two peaks in the tanδ versus temperature plots for manganese doped derivatives MSLT-1 and MSLT-2 can easily be explained by proposing that the three types of dipoles are present in the interlayer space one due the substitution of manganese ions as Mn^{3+} at Ti^{4-} site for lower doping and two types of dipoles due to the substitution of Mn^{2+} at two interlayer crystallographic alkali site Na/Li(1) and Na/Li(2) which create the necessary vacancy at the nearby alkali sites for higher doping as already reported in literature.[9,48,49] The ion vacancy (I-V) pairs so obtained would orient in all possible direction with respect to the applied field causes to increase in values of tanδ. The shifting of relaxation peaks towards higher temperature and then towards lower temperature due to the change in relaxation time and disorder introduced into the lattice.

As the concentration increases, the number of relaxations peaks increases but for derivative with higher doping the relaxations, peaks do not occur may be due to the participation of ions in the relaxation polarization, which grows with rise in temperature. The major role of manganese substitution at higher doping suppresses the relaxation peaks due to the permanent electric dipoles (5.0, 5.8 and 6.2D) (1Debye = 3.33564 X 10^{-30} cm.) present in the lattice.[39] The dependence of tanδ on frequency can explained with the help of equation given below

$$\text{Tan}\delta = \frac{\omega^2\tau^2(G_m + S) + G_m}{\omega[S\tau + C_g(\omega^2\tau^2 + 1)]}$$

where the symbols have their usual meanings. One can easily explain from this equation

$$\text{Lim.}_{\omega\to 0}\text{Tan}\delta = \infty$$

$$\text{Lim.}_{\omega\to\infty}\text{Tan}\delta = 0$$

The observed appreciable decrease in tanδ with rise in frequency at higher temperatures may be due to the accumulation of charges at interfaces in a multiphase material hence interfacial polarization (space charge polarization) takes place.[38,47] The low value of tanδ at higher frequencies is the outcome of the low reactance offered by ceramic sample. The higher rate of increase tanδ for low frequencies attributed to the space charge polarization.[38,47] At higher frequency sample offer low reactance to the sinusoidal signal and hence minimize the conduction losses, therefore the amount of dielectric losses are the characteristic of dipole mechanism and electrical conduction.

It is also found that the values of tanδ first decreases sharply up to 0.1 molar percentages doping of MnO_2 but increases slowly up to 1.0 molar percentage of MnO_2 up to 523K as shown in *Fig.* (3). As the temperature increases from 523K the tanδ increases sharply, this may be due to its molecular structure with the large losses due the dipole relaxation polarization as the relaxation peaks indicated in the high region. The decreased values of tanδ for the samples MSLT-1 and MSLT-2 suggest that the substitution of Mn^{3+} at Ti^{4+} site results

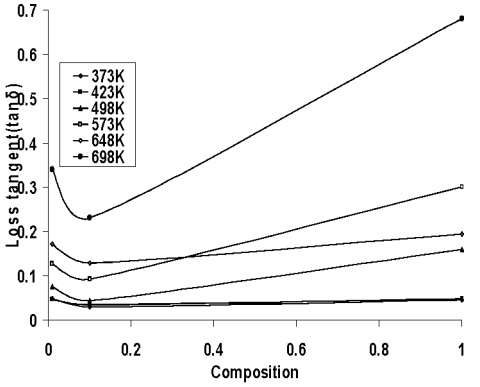

Fig. 3. Loss tangent (Tanδ) versus Composition for manganese doped derivatives

better configuration of the system in terms of losses. The increase in the values of tanδ again for the sample MSLT-3 in which the major amount of substitution occurs as Mn^{2+} at two interlayer crystallographic alkali site Na/Li(1) and Na/Li(2) furnish such a configuration of atoms which gives rise to increased values of tanδ.

The dependence of relative permittivity (ε_r) for MSLT-1, MSLT-2 and MSLT-3 on temperatures at certain fixed frequencies are shown in figure 4(a)-(c). The dependence of ε_r on temperature has approximately similar nature for sample MSLT-1 and MSLT-2 but entirely different nature for MSLT-3. The values of ε_r remains invariant up to the temperature 423K for MSLT-1, MSLT-2 and MSLT-3. After 423K the ε_r increases linearly with relaxation type peaks at 448K, 498K and 598K for MSLT-1 and 498K, 573K and 673K for MSLT-2. The shifting of peak may be due to the different roles of three types of dipoles generated due the substitution of manganese ions Mn^{3-} at Ti^{4+} sites and Mn^{2+} at two interlayer alkali sites. It can also be seen that ε_r continuously decreases as the frequency increases in higher temperature region. For MSLT-3 in *Fig.* 4(c), it can be seen that the values of ε_r suddenly decreases in numerical values. Its values lie in the range 20-30 up to 623K with a small resonant type peak at 448K. During the temperature range 623-648K ε_r strongly dependent on temperature but beyond 648K again ε_r has invariance nature up to the temperature range of study. The presence of resonant type peaks already discussed above.

The nature of dependence of relative permittivity may be different in solid ionic (linear i. e. not ferroelectric) dielectric. In most of the cases, an ionic mechanism of polarization increases ε_r when temperature grows. However, in some cases, the values of ε_r may diminish when temperature rises, particularly in those substances in which the ionic displacement intensifies the internal field and thereby the electronic polarization.[38] The molecules cannot orient themselves in the polar dielectric in the low temperature region, when temperature raises the orientation of the dipoles is facilitated and increases the dielectric constant. As the temperature grows the chaotic thermal oscillation of the molecules intensified and degree of orderliness of their orientation diminished. This causes the curves of dependence ε_r to pass through maximum and then drops. Mainly two factors are re-

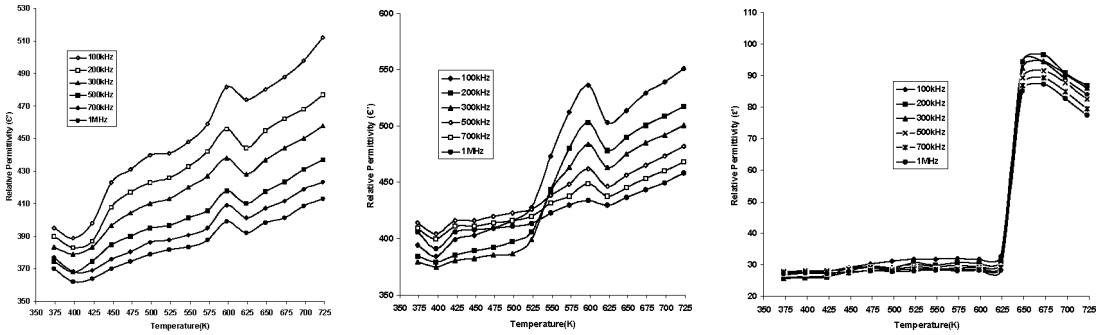

Fig. 4. (a) Relative Permittivity (ε') versus temperature for MSLT-1. (b) Relative Permittivity (ε') versus temperature for MSLT-2. (c) Relative Permittivity (ε') versus temperature for MSLT-3

sponsible for sudden fall in the values of ε_r for heavily doped derivative and further at 623K it again increases up to 648K becomes three times larger then the values of ε_t. Firstly, the decrease in values of ε_t up to 623K for MSLT-3 from MSLT-1 and MSLT-2 may be due to manganese ions inhibit the effect of Ti ions and the number of space charge carriers decreases leading to a lower polarization and hence a lower dielectric constant. Secondly, between the temperatures range 623-648K the vales of ε_r an increase three times it may be due to substitution of manganese ions at interlayer alkali sites. This will cause the dilation of interlayer space and simultaneously ε_t increases. As the frequency increases ε_r continuously decreases linearly from 523-723K for MSLT-1 and 573-723K for MSLT-2. The observed dispersion in ε_r frequency relation

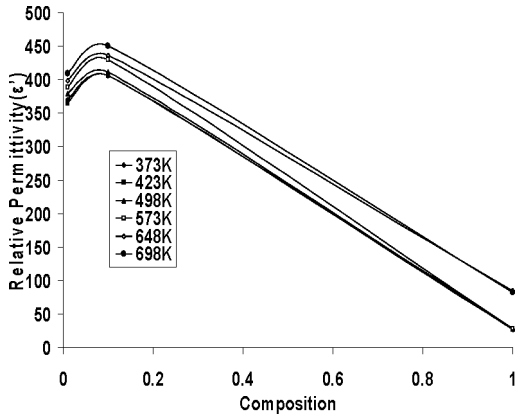

Fig. 5. Relative Permittivity (ε') versus Composition for manganese doped derivatives

can be explained on the basis of Maxwell Wagner model, in which the solid is assumed as composed of well conducting grains separated by poorly conducting grain boundary. The decrease in relative permittivity with divalent ion doping addition, according to Mc-Chesney et al.[40] and Cook and Tennery[41] was attributed to the formation of weak layers at the grain boundaries of the base matrix $Na_{1.9}Li_{0.1}Ti_3O_7$. These boundary layers are assumed compositionally different from the interior of the grain and may arise because of reaction between Mn ions and $Na_{1.9}Li_{0.1}Ti_3O_7$ or may originate from (Mn-Na/Li-Ti) complex oxide segregation at the grain boundaries.

Fig. 5 shows the dependence of ε_r on manganese concentration. It is found that ε_r first increases up to 0.1 molar percentage of MnO_2 and then suddenly decreases up to 1.0 molar percentage of MnO_2. The corresponding increase in the values of relative permittivity may be due to increase in number of dipoles in the interlayer space while the corresponding decrease in the values of relative permittivity may be due to the increase in the leakage current due to the higher doping.

Fig. 6(a)-(c) show the $\ln\sigma T(\Omega^{-1}m^{-1}K)$ versus $1000/T(K^{-1})$ plots for MSLT-1, MSLT-2 and MSLT-3. These curves are divided into three regions namely region I, II and III.

Region I (Lower temperature region)

The strongly frequency dependent and almost temperature independent region exists up to 598K

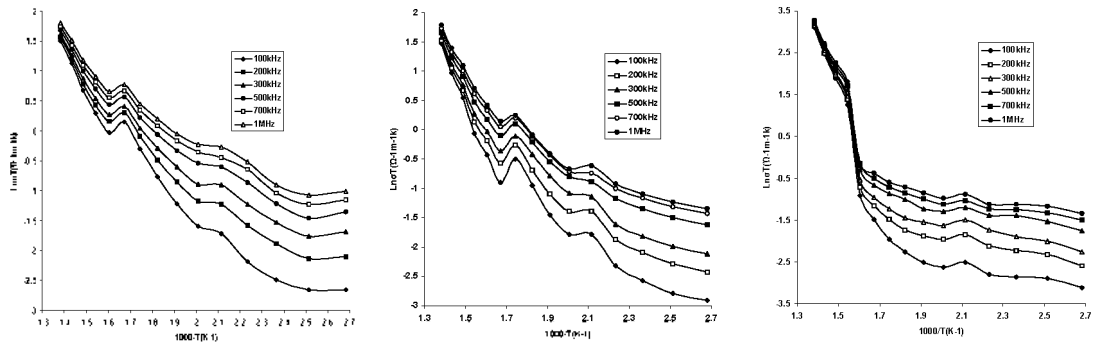

Fig. 6. (a) $Ln\sigma_{ac}T$ versus $1000/T\ (K^{-1})$ for MSLT-1. (b) $Ln\sigma_{ac}T$ versus $1000/T(K^{-1})$ for MSLT-2. (c) $Ln\sigma_{ac}T$ versus $1000/T(K^{-1})$ for MSLT-3

for MSLT-1, 573K for MSLT-2 and 623K for MSLT-3 with a small peak at 448K for MSLT-1 and MSLT-2, at 473K for MSLT-3. In ionic host lattices, where the interaction between orbital of neighboring ions, there is polarization of lattice associated with the presence of electronic carriers, the associated consisting of electronic carriers plus its polarization field is referred as polaron. Two types of polarons play a major role in conduction process at relatively lower temperature region. When the association is weak (large polarons), conductivity is similar to quasi-free electrons result with the small effective mass. When the electronic carrier plus the lattice distortion has the linear dimension smaller than the lattice parameter, it referred to as a small polaron, and the mobility is strongly affected by the lattice distortion which must move along with the electronic carrier. The loosened electrons from the negative ions and from the impurities in the crystal transported through the solid and would contribute to the conduction.[42] The polaron is an electron that always moves around together with the associated lattice polarization that minimizes its energy.[43] The nature of a. c. conductivity can be interpreted by proposing that the electronic hopping conduction, in which the hopping of electrons through shallow barrier along Ti-Ti chain take part in conduction. These electrons play a major role in this region. Such a frequency dependence of conductivity attributed to a wide distribution of relaxation times due to barrier height.[44] This region is very identical with those reported in conductivity plots of vacuum deposited ZnPc and CoPc thin film.[45] The conduction mechanism for the low temperature region can expressed as[46]

$$\sigma = \sigma_0 \exp[(-T_0/T)^{1/4}] \quad (1)$$

Region II (Mid temperature region)

This region exist from 598Kto 623K for MSLT-1, 573K to 598K for MSLT-2 and 623K to 648K for MSLT-3. It seen that in this temperature region the conductivity value has decreased with increasing temperature but suddenly increases for MSLT-3. The conduction mechanism in this region has been formulated by proposing that the loose oxygen's produced by the substitution of Mn^{3+} at Ti^{4+} will be trapped by cation vacancies present in the interlayer space leading to decrease in the conductivity. In this region, it found that no frequency dependence for MSLT-3 is seen in conductivity plots. It suggests that the electronic hopping conduction is still strongly contributing up to this higher temperature region for MSLT-1 and MSLT-2 but it is totally suppressed in sample MSLT-3 probably due to the reduction in the population of trapped electrons with the substitution of Mn^{2+} at interlayer alkali sites.

So the conduction mechanism for MSLT-1 and MSLT-2 may be hindered interlayer ionic conduction and electronic hopping conduction. The sudden increase in conductivity values between temperature range 623-648K has already discussed in (ε_r –T plots). The slope of conductivity plots is higher then intrinsic region for MSLT-3 so the mechanism of conduction for MSLT-3 attributed due to associated interlayer ionic conduction.

Region III (Higher temperature region)

Almost temperature dependent and very less frequency dependent region exist from 623K for MSLT-1, from 598K for MSLT-2 and from 648K for MSLT-3 up to the temperature range of study. The dependence of conductivity upon the frequency persists for manganese-doped derivatives for MSLT-1 and MSLT-2. The electronic contribution is less than the total conduction in the higher temperature region showing that at higher temperatures the conduction is mainly ionic. Accordingly, the conduction mechanism in this region may modified interlayer ionic conduction along with the polaronic conduction for MSLT-1 and MSLT-2 while only modified interlayer ionic conduction for MSLT-3. From these curves, it is clear that the dependence of ac conductivity decreases with increase in temperature. The frequency dependence of conductivity is the characteristic of electron hopping conduction, which decreases with rise in temperature, indicating a decrease in electron hop-

ping conduction and an increase in interlayer ionic conduction.

Fig. 7 shows the dependence of ln엯T($\Omega^{-1}m^{-1}K$) on composition. The conductivity first decreases up to 0.1 molar percentage of MnO_2 and sharply decreases up to for 1.0molar percentage of MnO_2. This may be due to the loosen electrons from $Ti_3O_7^{2-}$ that takes part in conduction process while at higher doping loosen oxygens are responsible for decrease in ac conductivity.

CONCLUSIONS

Dielectric-Spectroscopic investigations show dipole relaxation polarization along with the losses due to the motion of loosely bound ions and space charge polarization at higher temperature.

Three types of manganese substitutions and dipoles in the interlayer space as Mn^{3-} at Ti^{4+} site for lower doping and two types of dipoles due to the substitution of Mn^{2-} at two interlayer crystallographic alkali site Na/Li(1) and Na/Li(2) which create the necessary vacancy at the nearby alkali sites for higher doping have been identified through tanδ versus temperature plots for all the doped derivatives.

The dependency of relative permittivity on temperature and frequency for mixed ionic-electronic material Layered ($Na_{1.9}Li_{0.1}Ti_3O_7$) ceramic with 0.01, 0.1 and 1.0 molar percentage of MnO_2 doped derivatives indicates that the increase in the values of relative permittivity is due to increase in number of dipoles in the interlayer space. The corresponding decrease in the values of relative permittivity is due to the increase in the leakage current due to the higher doping.

A. C. Conductivity measurements pointed out that in intrinsic region only polaronic conduction exists for all manganese-doped derivatives. In extrinsic region the conduction mechanism for lower manganese-doped derivatives may hindered interlayer ionic conduction with electronic hopping conduction. The mechanism of conduction in heavily doped derivatives may be attributed due to associated interlayer ionic conduction and in ionic region the conduction mechanism in this region is modified interlayer ionic conduction along with the polaronic conduction for lower manganese doped derivatives while only modified interlayer ionic conduction for heavily doped derivatives.

Two types of polarons play a major role in conduction process at relatively lower temperature region. When the association is weak (large polarons), conductivity is similar to quasi-free electrons result with the small effective mass. When the electronic carrier plus the lattice distortion has the linear dimension smaller than the lattice parameter, it is referred to as a small polaron.

REFERENCE

1. S. Anderson and A. D. Wadsley, *Acta Crystallographic*, **1961,** *14*, 1245
2. S. Anderson and A. D. Wadsley, *Acta Crystallographic*, **1962**, *15*, 194
3. O. V. Yakubovich and V.V. Kireev, *Crystallographic Reports*, **2003**, *48*(1), 24
4. Shuji Ogura, Mitsuru Kohno, Kazunori Sato and Yasunobu Inoue, *J. Material Chem.* **1998**, *8(11)*, 2335
5. A. L. Sauvet, S. Baliteau, C. Shopez and P. Fabry, *J. Solid State Chem.* **2004**, *177*, 4508
6. M. Machida, X. W. Ma, H.Taniguchi, J. Yabunaka J.Kijima *J. Mol. Catal. A: Chem.* **2000**,*155*, 131
7. S. Kikkawa, F. Yasuda, M. Koizumi, *Mater. Res. Bull.* **1985,** *20*, 1221.
8. Shripal Prem Chand, and S.D. Pandey, .Solid state communications, **1989**, *69*(12), 1203.
9. Shripal, Prem Chand, S. D. Panday. *J. Mater. Sci.: Materials in Electronics* **1991**, *2* 89
10. Shripal, A. K. Mishra, S.D.Panday and R. P. Tandon, *Eur. J. Solid State Inorg. Chem.* **1992**, *29*, 229.
11. Shripal, R. P. Tandon and S.D. Panday, *J. Phys. Chem. Solids* **1991**, *52*(9), 1101.
12. Shripal, Sugandha Badhwar, Deepam Maurya, Jitendra Kumar, *J. Mater. Sci.: Materials in Electronics* **2005**, *16*, 495.
13. Shripal, Deepam Maurya, Shalini and Jitendra Kumar, *Material Sci. and Engineering B*, **2007** *136*, 5.
14. Deepam Maurya, Jitendra Kumar, Shripal, *J. Phys. Chem. Solids*, **2005**, *66*, 1614.
15. Shripal Sugandha Badhwar, Deepam Maurya, Jitendra Kumar and R. P. Tandon, *Advances in Condensed*

Matter Physics, edited by K. K. Rana (Allied Publisher, New Delhi) **2005**, 250.
16. D.Pal, R. P.Tandon and Shripal, *Indian Journal of Pure and Applied Physics*, **2006**, *44*(6), 435.
17. D. Pal, Prem Chand, R. P. Tandon and Shripal, *JKCS* **2005**, *49*(6), 560.
18. T. Sasaki, M. Watanabe, Y. Komatsu and Y. Fujiki, *Inorg. chem.* **1985**, *24*, 2265.
19. H. Izawa, S. Kikkawa, M. Koizumi, *J. Solid State Chem.* **1987**, *69*, 336.
20. H. Izawa, S. Kikkawa, M. Koizumi, *J. Solid State Chem.* **1985**, *60*, 269.
21. H. Izawa, S. Kikkawa, M. Koizumi, Polyhedron **1983**, *2*, 741.
22. N. Shinizuand M. Nakanishi, Japan Patent Kokai Tokkyo Koho *JP01*, **1989**, *249*, 38.
23. M. Koizumi, S. Yoshikawa and H. Izawa., Japan Patent Kokai Tokkyo Koho JP62, **1987**, *100*, 411.
24. M. W. Anderson and J. Klinowaski, *Inorg. Chem.* **1990**, *29*, 3260.
25. W. H. Hou, Q. J. Yan and X. C. Fu, *J. Chem. Soc. Chem. Communication*, **1994** 1371.
26. C. X. Guo W. H. Hou, M. Gou, Q. J. Yan and Y. Chen, *J. Chem. Soc. Chem. Communication (Cambridge)* **1997**, 801.
27. T. Chen, W. H. Hou, C. X. Guo, O. J. Yan and Y. Chen, *J. Chem. Soc. Dalton Trans.* **1997**, *92*, 359.
28. T. Sato, Y. Yamamoto, Y. Fujishiro and S. Uchida, *J. Chem. Soc. Faradey Trans.* **1996**, *92*, 5089.
29. S. Cheng and T. C. Wang, *J. Inorg. Chem.* **1989**, *28*, 1283.
30. J. N. Kondo, S. Shibata, Y. Ebina, K. Domen and A. Tanaka, J. Phys. Chem. **1995**, *99*, 16043.
31. M. Holzinger, A. Benisek, W. Schnelle, E. Gmelin, J. Maier and W. Sitte, J. Chem. Thermodynamics, **2003**, *35*, 1469.
32 K. J. Range, H. Fisher, F. Ketterl, S. Afr. *J. Chem.* **1987**, *40*, 233.
33. A. D. Wadsley, W. G. Mumme, Acta Cryst. B24 **1968**, 392.
34. M. Dion, Y. Piffard, M. Tournoux, J. Inorg. Nucl. Chem. **1967**, *40*(12), 1442.
35. V. B. Nalbandyan, I. L. Shukaev, Z. Neorgam, Khimii, Russian *J. Inorg. Chem.* **1990**, *35*, 1085.
36. M. Sh. Khalil and F. F. Hammad, *Egypt. J. Sol.* **2002**, *25*(2), 1-9.
37. Seoung-soo Lee and Song-Ho Beyon, *Bull. Korean Chemical Society*, 2004, *25*(4),1051-1054.
38. B. Tareev, *Physics of Dielectric Materials, Mir Publishers, Moscow*, (1979) Ch.3.
39. S. Ogura, K. Soto and Y. Inoue, *J. Phys. Chem. Chem. Phys.* 2002, *2*, 2449.
40. J.B. MacChesney et al. *J. Am. Ceam. Soc.* **1963**, *46*(5), 197.
41. R. L. Cook and V. J. Tennery, J. Am. Ceram. Soc., **1961**, *44*(4), 187.
42. H. Inokuchi, *Solid State Physics, edited by L. Jacob, Dover Publications, USA*,**1965**, 45.
43. David Adler, *The Imperfect SolidTransport Properties Treatise in Solid State Chemistry, Edited by N. B. Hanny, Plenum Press, USA*, **1975**, 237-321.
44. G. E. Pike, *Phys. Rev. B* **1972**, *6*, 1571.
45. R. K. Rajesh and C. S. Menon *Indian journal of Pure and applied physics*, **2005**, *43*, 964.
46. Shklovskii B. I. and Efros A. L., Electronic properties of doped semiconductors (Springler, Berlin), **1984**.
47. B. P. Das, R. N. P. Choudhary and P. K. Mahapatra, *Mater. Sci. Eng. B* **2003**, 104 96.
48. D.Pal, Shripal, *J. Mater. Sci.: Materials in Electronics* **2007**, *18*, 401.
49. Dharmendra Pal, Prem Chand and Shripal, *Proceeding of NSFD-XIII*, **2004**, 39.
50. Alka Tangri, Pradeep Mishra, D. Pal, *Int. J. Chem. Sci.* **2005**, 3(4), 715-720.